Available online at www.sciencedirect.com
ScienceDirect
Composite Structures 77 (2007) 97–103
COMPOSITE STRUCTURES
www.elsevier.com/locate/compstruct

The behavior of two parallel interface cracks in magneto–electro–elastic materials under an anti-plane shear stress loading

Zhen-Gong Zhou [a], Yuan Chen [b,*], Biao Wang [a]

[a] P.O. Box 3010, Center for Composite Materials, Harbin Institute of Technology, Harbin 150080, PR China
[b] Zhengzhou University, Zhengzhou 450052, PR China

Available online 15 September 2006

Abstract

In this paper, the behavior of two parallel symmetry interface cracks in magneto–electro–elastic materials under an anti-plane shear stress loading is studied by Schmidt method. By using the Fourier transform, the problem can be solved with a pair of dual integral equations in which the unknown variables are the jumps of the displacements across the crack surfaces. To solve the dual integral equations, the jumps of the displacements across the crack surfaces are expanded in a series of Jacobi polynomials. The relations among the electric filed, the magnetic flux and the stress field are obtained. The shielding effect of two parallel interface cracks has been discussed.

Keywords: Magneto–electro–elastic materials; Interface crack; Dual integral equations

1. Introduction

The piezoelectric–piezomagnetic materials are a sort of multi-functionally materials. The piezoelectric–piezomagnetic materials possess piezoelectric, piezomagnetic and magneto-electric effects, thereby making the composite sensitive to elastic, electric and magnetic fields. Consequently, they are extensively used as electric packaging, sensors and actuators, e.g., magnetic field probes, acoustic/ultrasonic devices, hydrophones, and transducers with the responsibility of electro–magneto–mechanical energy conversion [1]. When subjected to mechanical, magnetic and electrical loads in service, these magneto–electro–elastic composites can fail prematurely due to some defects, e.g., cracks, holes, etc. arising during their manufacturing processes. Therefore, it is of great importance to study the magneto–electro–elastic interaction and fracture behaviors of magneto–electro–elastic materials [2–7]. Liu et al. [8] studied the generalized 2D problem of an infinite magneto–electro–elastic plane with an elliptical hole. Gao et al. [9,10] and Wang and Mai [11] also studied the fracture problem of the piezoelectric–piezomagnetic composites. The development of piezoelectric–piezomagnetic composites has its roots in the early work of Van Suchtelen [12] who proposed that the combination of piezoelectric–piezomagnetic phases may exhibit a new material property—the magnetoelectric coupling effect. Since then, there have not been many researchers studying magnetoelectric coupling effect in $BaTiO_3$–$CoFe_2O_4$ composites, and most research results published were obtained in recent years [1–10,13–18]. The static fracture behavior of two parallel symmetry interface cracks in the piezoelectric materials has been investigated in Ref. [19]. However, to our knowledge, the behavior of magneto–electro–elastic materials with two parallel symmetry interface cracks subjected to anti-plane shear stress loading has not been studied by using the Schmidt method [20,21]. Thus, the present work is an attempt to fill this information needed.

In this paper, the behavior of two parallel symmetry interface cracks in magneto–electro–elastic material plane subjected to anti-plane shear loading is investigated by use

* Corresponding author.
E-mail addresses: zhouzhg@hit.edu.cn (Z.-G. Zhou), chenyuan@zzu.edu.cn (Y. Chen).

0263-8223/$ - see front matter © 2005 Published by Elsevier Ltd.
doi:10.1016/j.compstruct.2005.11.056

of the Schmidt method [20,21]. The Fourier transform is applied and a mixed boundary value problem is reduced to a pair of dual integral equations. To solve the dual integral equations, the jumps of the displacements across the crack surfaces are expanded in a series of Jacobi polynomials. This process is quite different from those adopted in Refs. [2–11] as mentioned above. The present problem is also quite different from the problem in Ref. [19]. Only the electro–elastic coupling effects were considered in Ref. [19]. Numerical solutions are obtained for the stress. The shielding effect of two parallel interface cracks has been discussed.

2. Formulation of the problem

Fig. 1 shows a piezoelectric–piezomagnetic material layered structure made by bonding together with two same half planes. The piezoelectric–piezomagnetic material layer is layer 2 of thickness h, with two parallel interface cracks of length $2l$ created. A Cartesian coordinate system (x, y) is positioned as shown in Fig. 1. The piezoelectric–piezomagnetic boundary-value problem for anti-plane shear is considerably simplified if we consider only the out-of-plane displacement, the in-plane electric fields and the in-plane magnetic fields. As discussed in Soh et al.'s [22] works, since no opening displacement exists for the present anti-plane problem, the crack surfaces can be assumed to be in perfect contact. Accordingly, the electric potential, the magnetic potential, the normal electric displacement and the normal magnetic flux are assumed to be continuous across the crack surfaces. Here, the standard superposition technique is used and only the perturbation fields are considered in the present paper. So the boundary conditions of the present problem are

$$\begin{cases} \tau_{yz}^{(1)}(x,h^+)=\tau_{yz}^{(2)}(x,h^-)=-\tau_0, & |x|\leqslant l \\ w^{(1)}(x,h^+)=w^{(2)}(x,h^-), & |x|>l \\ \tau_{yz}^{(2)}(x,0^+)=\tau_{yz}^{(3)}(x,0^-)=-\tau_0, & |x|\leqslant l \\ w^{(2)}(x,0^+)=w^{(3)}(x,0^-), & |x|>l \end{cases} \tag{1}$$

$$\begin{cases} \phi^{(1)}(x,h^+)=\phi^{(2)}(x,h^-), \quad D_y^{(1)}(x,h^+)=D_y^{(2)}(x,h^-), \ |x|<\infty \\ \psi^{(1)}(x,h^+)=\psi^{(2)}(x,h^-), \quad B_y^{(1)}(x,h^+)=B_y^{(2)}(x,h^-), \ |x|<\infty \end{cases} \tag{2}$$

$$\begin{cases} \phi^{(2)}(x,0^+)=\phi^{(3)}(x,0^-), \quad D_y^{(2)}(x,0^+)=D_y^{(3)}(x,0^-), \ |x|<\infty \\ \psi^{(2)}(x,0^+)=\psi^{(3)}(x,0^-), \quad B_y^{(2)}(x,0^+)=B_y^{(3)}(x,0^-), \ |x|<\infty \end{cases} \tag{3}$$

$$w^{(1)}(x,y)=w^{(2)}(x,y)=w^{(3)}(x,y)=0 \quad \text{for } (x^2+y^2)^{1/2}\to\infty \tag{4}$$

where $\tau_{zk}^{(i)}$, $D_k^{(i)}$ and $B_k^{(i)}$ $(k=x,y,\ i=1,2,3)$ are the anti-plane shear stress, in-plane electric displacement and in-plane magnetic flux, respectively. $w^{(i)}$, $\phi^{(i)}$ and $\psi^{(i)}$ are the mechanical displacement, the electric potential and the magnetic potential. Also note that all quantities with superscript i $(i=1,2,3)$ refer to the upper half plane 1, the layer 2 and the lower half plane 3 as shown in Fig. 1, respectively. In this paper, we only consider that τ_0 is positive.

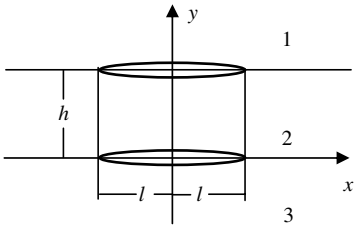

Fig. 1. Two parallel symmetry interface cracks in magneto–electro–elastic materials.

It is assumed that the magneto–electro–elastic material is transversely isotropic. So the constitutive equations for the mode III crack in the magneto–electro–elastic material can be expressed as

$$\tau_{zk}^{(i)}=c_{44}^{(i)}w_{,k}^{(i)}+e_{15}^{(i)}\phi_{,k}^{(i)}+q_{15}^{(i)}\psi_{,k}^{(i)} \quad (k=x,y,\ i=1,2,3) \tag{5}$$

$$D_k^{(i)}=e_{15}^{(i)}w_{,k}^{(i)}-\varepsilon_{11}^{(i)}\phi_{,k}^{(i)}-d_{11}^{(i)}\psi_{,k}^{(i)} \quad (k=x,y,\ i=1,2,3) \tag{6}$$

$$B_k^{(i)}=q_{15}^{(i)}w_{,k}^{(i)}-d_{11}^{(i)}\phi_{,k}^{(i)}-\mu_{11}^{(i)}\psi_{,k}^{(i)} \quad (k=x,y,\ i=1,2,3) \tag{7}$$

where $c_{44}^{(i)}$ is shear modulus, $e_{15}^{(i)}$ is piezoelectric coefficient, $\varepsilon_{11}^{(i)}$ is dielectric parameter, $q_{15}^{(i)}$ is piezomagnetic coefficient, $d_{11}^{(i)}$ is electromagnetic coefficient, $\mu_{11}^{(i)}$ is magnetic permeability, where $c_{44}^{(1)}=c_{44}^{(3)}$, $e_{15}^{(1)}=e_{15}^{(3)}$, $\varepsilon_{11}^{(1)}=\varepsilon_{11}^{(3)}$, $q_{15}^{(1)}=q_{15}^{(3)}$, $d_{11}^{(1)}=d_{11}^{(3)}$ and $\mu_{11}^{(1)}=\mu_{11}^{(3)}$.

The anti-plane governing equations are

$$c_{44}^{(i)}\nabla^2w^{(i)}+e_{15}^{(i)}\nabla^2\phi^{(i)}+q_{15}^{(i)}\nabla^2\psi^{(i)}=0 \quad (i=1,2,3) \tag{8}$$

$$e_{15}^{(i)}\nabla^2w^{(i)}-\varepsilon_{11}^{(i)}\nabla^2\phi^{(i)}-d_{11}^{(i)}\nabla^2\psi^{(i)}=0 \quad (i=1,2,3) \tag{9}$$

$$q_{15}^{(i)}\nabla^2w^{(i)}-d_{11}^{(i)}\nabla^2\phi^{(i)}-\mu_{11}^{(i)}\nabla^2\psi^{(i)}=0 \quad (i=1,2,3) \tag{10}$$

where $\nabla^2=\partial^2/\partial x^2+\partial^2/\partial y^2$ is the two-dimensional Laplace operator. Because of the assumed symmetry in geometry and loading, it is sufficient to consider only the problem for $0\leqslant x<\infty$, $-\infty\leqslant y<\infty$. A Fourier transform is applied to Eqs. (8)–(10). It is assumed that the solutions are

$$\begin{cases} w^{(1)}(x,y)=\frac{2}{\pi}\int_0^\infty A_1(s)\mathrm{e}^{-sy}\cos(sx)\mathrm{d}s \\ \phi^{(1)}(x,y)=\frac{a_1}{a_0}w^{(1)}(x,y)+\frac{2}{\pi}\int_0^\infty B_1(s)\mathrm{e}^{-sy}\cos(sx)\mathrm{d}s \quad (y\geqslant h) \\ \psi^{(1)}(x,y)=\frac{a_2}{a_0}w^{(1)}(x,y)+\frac{2}{\pi}\int_0^\infty C_1(s)\mathrm{e}^{-sy}\cos(sx)\mathrm{d}s \end{cases} \tag{11}$$

$$\begin{cases} w^{(2)}(x,y)=\frac{2}{\pi}\int_0^\infty[A_2(s)\mathrm{e}^{-sy}+B_2(s)\mathrm{e}^{sy}]\cos(sx)\mathrm{d}s \\ \phi^{(2)}(x,y)=\frac{a_4}{a_3}w^{(2)}(x,y)+\frac{2}{\pi}\int_0^\infty[C_2(s)\mathrm{e}^{-sy} \\ \qquad +D_2(s)\mathrm{e}^{sy}]\cos(sx)\mathrm{d}s \qquad (0\leqslant y\leqslant h) \\ \psi^{(3)}(x,y)=\frac{a_5}{a_3}w^{(2)}(x,y)+\frac{2}{\pi}\int_0^\infty[E_2(s)\mathrm{e}^{-sy} \\ \qquad +F_2(s)\mathrm{e}^{sy}]\cos(sx)\mathrm{d}s \end{cases} \tag{12}$$

$$\begin{cases} w^{(3)}(x,y)=\frac{2}{\pi}\int_0^\infty A_3(s)\mathrm{e}^{sy}\cos(sx)\mathrm{d}s \\ \phi^{(3)}(x,y)=\frac{a_1}{a_0}w^{(3)}(x,y)+\frac{2}{\pi}\int_0^\infty B_3(s)\mathrm{e}^{sy}\cos(sx)\mathrm{d}s \quad (y\leqslant 0) \\ \psi^{(3)}(x,y)=\frac{a_2}{a_0}w^{(3)}(x,y)+\frac{2}{\pi}\int_0^\infty C_3(s)\mathrm{e}^{sy}\cos(sx)\mathrm{d}s \end{cases} \tag{13}$$

where $a_0 = \varepsilon_{11}^{(1)}\mu_{11}^{(1)} - d_{11}^{(1)2}$, $a_1 = \mu_{11}^{(1)}e_{15}^{(1)} - d_{11}^{(1)}q_{15}^{(1)}$, $a_2 = q_{15}^{(1)}\varepsilon_{11}^{(1)} - d_{11}^{(1)}e_{15}^{(1)}$, $a_3 = \varepsilon_{11}^{(2)}\mu_{11}^{(2)} - d_{11}^{(2)2}$, $a_4 = \mu_{11}^{(2)}e_{15}^{(2)} - d_{11}^{(2)}q_{15}^{(2)}$, $a_5 = q_{15}^{(2)}\varepsilon_{11}^{(2)} - d_{11}^{(2)}e_{15}^{(2)}$. $A_1(s)$, $B_1(s)$, $C_1(s)$, $A_2(s)$, $B_2(s)$, $C_2(s)$, $D_2(s)$, $E_2(s)$, $F_2(s)$, $A_3(s)$, $B_3(s)$ and $C_3(s)$ are unknown functions.

So from Eqs. (5)–(7), we have

$$\tau_{yz}^{(1)}(x,y) = -\frac{2}{\pi}\int_0^\infty s\left[\left(c_{44}^{(1)} + \frac{a_1e_{15}^{(1)}}{a_0} + \frac{a_2q_{15}^{(1)}}{a_0}\right)A_1(s) + e_{15}^{(1)}B_1(s) + q_{15}^{(1)}C_1(s)\right]e^{-sy}\cos(sx)\mathrm{d}s \tag{14}$$

$$D_y^{(1)}(x,y) = \frac{2}{\pi}\int_0^\infty s[\varepsilon_{11}^{(1)}B_1(s) + d_{11}^{(1)}C_1(s)]e^{-sy}\cos(sx)\mathrm{d}s \tag{15}$$

$$B_y^{(1)}(x,y) = \frac{2}{\pi}\int_0^\infty s[d_{11}^{(1)}B_1(s) + \mu_{11}^{(1)}C_1(s)]e^{-sy}\cos(sx)\mathrm{d}s \tag{16}$$

$$\tau_{yz}^{(2)}(x,y) = -\frac{2}{\pi}\int_0^\infty s\left\{\left[\left(c_{44}^{(2)} + \frac{a_4e_{15}^{(2)}}{a_3} + \frac{a_5q_{15}^{(2)}}{a_3}\right)A_2(s) + e_{15}^{(2)}C_2(s) + q_{15}^{(2)}E_2(s)\right]e^{-sy} - \left[\left(c_{44}^{(2)} + \frac{a_4e_{15}^{(2)}}{a_3} + \frac{a_5q_{15}^{(2)}}{a_3}\right) \times B_2(s) + e_{15}^{(2)}D_2(s) + q_{15}^{(2)}F_2(s)\right]e^{sy}\right\}\cos(sx)\mathrm{d}s \tag{17}$$

$$D_y^{(2)}(x,y) = \frac{2}{\pi}\int_0^\infty s\{[\varepsilon_{11}^{(2)}C_2(s) + d_{11}^{(2)}E_2(s)]e^{-sy} - [\varepsilon_{11}^{(2)}D_2(s) + d_{11}^{(2)}F_2(s)]e^{sy}\}\cos(sx)\mathrm{d}s \tag{18}$$

$$B_y^{(2)}(x,y) = \frac{2}{\pi}\int_0^\infty s\{[d_{11}^{(2)}C_2(s) + \mu_{11}^{(2)}E_2(s)]e^{-sy} - [d_{11}^{(2)}D_2(s) + \mu_{11}^{(2)}F_2(s)]e^{sy}\}\cos(sx)\mathrm{d}s \tag{19}$$

$$\tau_{yz}^{(3)}(x,y) = \frac{2}{\pi}\int_0^\infty s\left[\left(c_{44}^{(1)} + \frac{a_1e_{15}^{(1)}}{a_0} + \frac{a_2q_{15}^{(1)}}{a_0}\right)A_3(s) + e_{15}^{(1)}B_3(s) + q_{15}^{(1)}C_3(s)\right]e^{sy}\cos(sx)\mathrm{d}s \tag{20}$$

$$D_y^{(3)}(x,y) = -\frac{2}{\pi}\int_0^\infty s[\varepsilon_{11}^{(1)}B_3(s) + d_{11}^{(1)}C_3(s)]e^{sy}\cos(sx)\mathrm{d}s \tag{21}$$

$$B_y^{(3)}(x,y) = -\frac{2}{\pi}\int_0^\infty s[d_{11}^{(1)}B_3(s) + \mu_{11}^{(1)}C_3(s)]e^{sy}\cos(sx)\mathrm{d}s \tag{22}$$

To solve the problem, the jumps of the displacements across the crack surfaces are defined as follows:

$$f_1(x) = w^{(1)}(x,h^+) - w^{(2)}(x,h^-) \tag{23}$$

$$f_2(x) = w^{(2)}(x,0^+) - w^{(3)}(x,0^-) \tag{24}$$

Substituting Eqs. (11)–(13) into Eqs. (23) and (24), applying the Fourier transform and the boundary conditions (2) and (3), it can be obtained

$$A_1(s)e^{-sh} - A_2(s)e^{-sh} - B_2(s)e^{sh} = \bar{f}_1(s),$$
$$A_2(s) + B_2(s) - A_3(s) = \bar{f}_2(s) \tag{25}$$

$$\frac{a_1}{a_0}A_1(s)e^{-sh} - \frac{a_4}{a_3}[A_2(s)e^{-sh} + B_2(s)e^{sh}] + B_1(s)e^{-sh} - C_2(s)e^{-sh} - D_2(s)e^{sh} = 0 \tag{26}$$

$$\frac{a_4}{a_3}[A_2(s) + B_2(s)] - \frac{a_1}{a_0}A_3(s) + C_2(s) + D_2(s) - B_3(s) = 0 \tag{27}$$

$$\frac{a_2}{a_0}A_1(s)e^{-sh} - \frac{a_5}{a_3}[A_2(s)e^{-sh} + B_2(s)e^{sh}] + C_1(s)e^{-sh} - E_2(s)e^{-sh} - F_2(s)e^{sh} = 0 \tag{28}$$

$$\frac{a_5}{a_3}[A_2(s) + B_2(s)] - \frac{a_2}{a_0}A_3(s) + E_2(s) + F_2(s) - C_3(s) = 0 \tag{29}$$

A superposed bar indicates the Fourier transform throughout the paper. Substituting Eqs. (14)–(22) into Eqs. (1)–(3), it can be obtained

$$[\delta^{(1)}A_1(s) + e_{15}^{(1)}B_1(s) + q_{15}^{(1)}C_1(s)]e^{-sh} - [\delta^{(2)}A_2(s) + e_{15}^{(2)}C_2(s) + q_{15}^{(2)}E_2(s)]e^{-sh} + [\delta^{(2)}B_2(s) + e_{15}^{(2)}D_2(s) + q_{15}^{(2)}F_2(s)]e^{sh} = 0 \tag{30}$$

$$\delta^{(2)}A_2(s) + e_{15}^{(2)}C_2(s) + q_{15}^{(2)}E_2(s) - [\delta^{(2)}B_2(s) + e_{15}^{(2)}D_2(s) + q_{15}^{(2)}F_2(s)] + [\delta^{(2)}A_3(s) + e_{15}^{(1)}B_3(s) + q_{15}^{(1)}C_3(s)] = 0 \tag{31}$$

$$-[\varepsilon_{11}^{(1)}B_1(s) + d_{11}^{(1)}C_1(s)]e^{-sh} + [\varepsilon_{11}^{(2)}C_2(s) + d_{11}^{(2)}E_2(s)]e^{-sh} - [\varepsilon_{11}^{(2)}D_2(s) + d_{11}^{(2)}F_2(s)]e^{sh} = 0 \tag{32}$$

$$-\varepsilon_{11}^{(2)}C_2(s) - d_{11}^{(2)}E_2(s) + \varepsilon_{11}^{(2)}D_2(s) + d_{11}^{(2)}F_2(s) - \varepsilon_{11}^{(1)}B_3(s) - d_{11}^{(1)}C_3(s) = 0 \tag{33}$$

$$[-d_{11}^{(1)}B_1(s) - \mu_{11}^{(1)}C_1(s)]e^{-sh} + [d_{11}^{(2)}C_2(s) + \mu_{11}^{(2)}E_2(s)]e^{-sh} - [d_{11}^{(2)}D_2(s) + \mu_{11}^{(2)}F_2(s)]e^{sh} = 0 \tag{34}$$

$$-d_{11}^{(2)}C_2(s) - \mu_{11}^{(2)}E_2(s) + d_{11}^{(2)}D_2(s) + \mu_{11}^{(2)}F_2(s)] - d_{11}^{(1)}B_3(s) - \mu_{11}^{(1)}C_3(s) = 0 \tag{35}$$

where $\delta^{(1)} = c_{44}^{(1)} + \frac{a_1e_{15}^{(1)}}{a_0} + \frac{a_2q_{15}^{(1)}}{a_0}$, $\delta^{(2)} = c_{44}^{(2)} + \frac{a_4e_{15}^{(2)}}{a_3} + \frac{a_5q_{15}^{(2)}}{a_3}$.

By solving twelve Eqs. (25)–(35) with twelve unknown functions $A_1(s)$, $B_1(s)$, $C_1(s)$, $A_2(s)$, $B_2(s)$, $C_2(s)$, $D_2(s)$, $E_2(s)$, $F_2(s)$, $A_3(s)$, $B_3(s)$ and $C_3(s)$ and applying the boundary conditions (1)–(2) to the results, it can be obtained

$$\frac{2}{\pi}\int_0^\infty \bar{f}_1(s)\cos(sx)\mathrm{d}s = 0, \quad x > l \tag{36}$$

$$\frac{2}{\pi}\int_0^\infty \bar{f}_2(s)\cos(sx)\mathrm{d}s = 0, \quad x > l \tag{37}$$

$$\frac{2}{\pi}\int_0^\infty s[g_1(s)\bar{f}_1(s) + g_2(s)\bar{f}_2(s)]\cos(sx)\mathrm{d}s = -\tau_0, \quad 0 \leqslant x \leqslant l \tag{38}$$

$$\frac{2}{\pi}\int_0^\infty s[g_2(s)\bar{f}_1(s) + g_1(s)\bar{f}_2(s)]\cos(sx)\mathrm{d}s = -\tau_0, \quad 0 \leqslant x \leqslant l \tag{39}$$

From Eqs. (36)–(39), it can be obtained

$$\bar{f}_1(s) = \bar{f}_2(s) \Rightarrow f_1(x) = f_2(x), \quad \tau_{yz}^{(1)}(x,h) = \tau_{yz}^{(2)}(x,h) = \tau_{yz}^{(2)}(x,0) = \tau_{yz}^{(3)}(x,0) \tag{40}$$

$$D_y^{(1)}(x,h) = D_y^{(2)}(x,h) = D_y^{(2)}(x,0) = D_y^{(3)}(x,0) \tag{41}$$

$$B_y^{(1)}(x,h) = B_y^{(2)}(x,h) = B_y^{(2)}(x,0) = B_y^{(3)}(x,0) \tag{42}$$

where $g_1(s)$ and $g_2(s)$ is a known function (see Appendix A). $\lim_{s\to\infty} g_1(s) = \beta_1$ and $\lim_{s\to\infty} g_2(s) = 0$, where β_1 is a constant that depends on the properties of the materials (see Appendix A). When the properties of the upper and the lower half planes is the same, $\beta_1 = -c_{44}^{(1)}/2$. To determine the unknown functions $\bar{f}_1(s)$ and $\bar{f}_2(s)$, the above two pairs of dual integral equations (36)–(39) must be solved.

3. Solution of the dual integral equations

From the natural property of the displacement along the crack line, it can be obtained that the jumps of the displacements across the crack surface are a finite, continuous and differentiable function. Hence, the jumps of the displacements across the crack surfaces can be represented by the following series:

$$f_1(x) = f_2(x) = \sum_{n=1}^{\infty} b_n P_{2n-2}^{\left(\frac{1}{2},\frac{1}{2}\right)}\left(\frac{x}{l}\right)\left(1-\frac{x^2}{l^2}\right)^{\frac{1}{2}}, \quad \text{for } 0 \leqslant x \leqslant l \tag{43}$$

$$f_1(x) = f_2(x) = w^{(1)}(x,h^+) - w^{(2)}(x,h^-) = 0, \quad \text{for } x > l \tag{44}$$

where b_n are unknown coefficients to be determined and $P_n^{(1/2,1/2)}(x)$ is a Jacobi polynomial [23]. The Fourier transform of Eqs. (43) and (44) is [24]

$$\bar{f}_1(s) = \sum_{n=1}^{\infty} b_n G_n \frac{1}{s} J_{2n-1}(sl), \qquad G_n = 2\sqrt{\pi}(-1)^{n-1}\frac{\Gamma\left(2n-\frac{1}{2}\right)}{(2n-2)!} \tag{45}$$

where $\Gamma(x)$ and $J_n(x)$ are the Gamma and Bessel functions, respectively.

Substituting Eq. (45) into Eqs. (36)–(39), respectively. It can be shown that Eqs. (36) and (37) are automatically satisfied. After integration with respect to x in $[0,x]$, Eqs. (38) and (39) reduce to

$$\frac{2}{\pi}\sum_{n=1}^{\infty} b_n G_n \int_0^{\infty} \frac{1}{s}[g_1(s)+g_2(s)]J_{2n-1}(sl)\sin(sx)\mathrm{d}s = -\tau_0 x \tag{46}$$

From the relationship [23]

$$\int_0^{\infty} \frac{1}{s} J_n(sa)\sin(bs)\mathrm{d}s = \begin{cases} \dfrac{\sin[n\sin^{-1}(b/a)]}{n} & a > b \\ \dfrac{a^n \sin(n\pi/2)}{n[b+\sqrt{b^2-a^2}]^n} & b > a \end{cases} \tag{47}$$

the semi-infinite integral in Eq. (46) can be modified as

$$\int_0^{\infty} \frac{1}{s}[g_1(s)+g_2(s)]J_{2n-1}(sl)\sin(sx)\mathrm{d}s = \frac{\beta_1}{2n-1}\sin\left[(2n-1)\sin^{-1}\left(\frac{x}{l}\right)\right] + \int_0^{\infty}\frac{1}{s}[g_1(s)+g_2(s)-\beta_1]J_{2n-1}(sl)\sin(sx)\mathrm{d}s \tag{48}$$

It can be seen that the integrands in the right end of Eq. (48) tend rapidly to zero. Thus the semi-infinite integrals in Eq. (48) can be numerical evaluated easily. Eq. (46) can now be solved for the coefficients b_n by the Schmidt method [20]. For brevity, Eq. (46) can be rewritten as

$$\sum_{n=1}^{\infty} b_n E_n(x) = U(x), \quad 0 \leqslant x \leqslant l \tag{49}$$

where $E_n(x)$ and $U(x)$ are known functions and the coefficients b_n are to be determined. A set of functions $P_n(x)$ which satisfy the orthogonality condition

$$\int_0^l P_m(x)P_n(x)\mathrm{d}x = N_n\delta_{mn}, \quad N_n = \int_0^l P_n^2(x)\mathrm{d}x \tag{50}$$

can be constructed from the function, $E_n(x)$, such that

$$P_n(x) = \sum_{i=1}^{n}\frac{M_{in}}{M_{nn}}E_i(x) \tag{51}$$

where M_{ij} is the cofactor of the element d_{ij} of D_n, which is defined as

$$D_n = \begin{bmatrix} d_{11}, d_{12}, d_{13}, \ldots, d_{1n} \\ d_{21}, d_{22}, d_{23}, \ldots, d_{2n} \\ d_{31}, d_{32}, d_{33}, \ldots, d_{3n} \\ \cdots \\ \cdots \\ \cdots \\ d_{n1}, d_{n2}, d_{n3}, \ldots, d_{nn} \end{bmatrix}, \quad d_{ij} = \int_0^l E_i(x)E_j(x)\mathrm{d}x \tag{52}$$

Using Eqs. (49)–(52), we obtain

$$b_n = \sum_{j=n}^{\infty} q_j \frac{M_{nj}}{M_{jj}} \quad \text{with } q_j = \frac{1}{N_j}\int_0^l U(x)P_j(x)\mathrm{d}x \tag{53}$$

4. Intensity factors

The coefficients b_n are known, so that the entire perturbation stress field, the perturbation electric displacement and the magnetic flux can be obtained. However, in fracture mechanics, it is of importance to determine the perturbation stress τ_{yz} and the perturbation electric displacement D_y in the vicinity of the crack tips. In the case of the present

study, $\tau_{yz}^{(1)}$, $\tau_{yz}^{(2)}$, $\tau_{yz}^{(3)}$, $D_y^{(1)}$, $D_y^{(2)}$, $D_y^{(3)}$, $B_y^{(1)}$, $B_y^{(2)}$ and $B_y^{(3)}$ along the crack line can be expressed respectively as

$$\tau_{yz}^{(1)}(x,h)=\tau_{yz}^{(2)}(x,h)=\tau_{yz}^{(2)}(x,0)=\tau_{yz}^{(3)}(x,0)=\tau_{yz}$$
$$=\frac{2}{\pi}\sum_{n=1}^{\infty}b_nG_n\int_0^{\infty}[g_1(s)+g_2(s)]J_{2n-1}(sl)\cos(xs)\mathrm{d}s \quad (54)$$

$$D_y^{(1)}(x,h)=D_y^{(2)}(x,h)=D_y^{(2)}(x,0)=D_y^{(3)}(x,0)=D_y$$
$$=\frac{2}{\pi}\sum_{n=1}^{\infty}b_nG_n\int_0^{\infty}g_3(s)J_{2n-1}(sl)\cos(xs)\mathrm{d}s \quad (55)$$

$$B_y^{(1)}(x,h)=B_y^{(2)}(x,h)=B_y^{(2)}(x,0)=B_y^{(3)}(x,0)=B_y$$
$$=\frac{2}{\pi}\sum_{n=1}^{\infty}b_nG_n\int_0^{\infty}g_4(s)J_{2n-1}(sl)\cos(xs)\mathrm{d}s \quad (56)$$

where $g_3(s)$ and $g_4(s)$ are known functions (see Appendix A). $\lim_{s\to\infty}g_3(s)=\beta_2$. $\lim_{s\to\infty}g_4(s)=\beta_3$, where β_2 and β_3 are two constants which depend on the properties of the materials (see Appendix A). When the properties of the upper and the lower half planes is the same, $\beta_2=-e_{15}^{(1)}/2$ and $\beta_3=-q_{15}^{(1)}/2$. From the relationship [23]

$$\int_0^{\infty}J_n(sa)\cos(bs)\mathrm{d}s=\begin{cases}\dfrac{\cos[n\sin^{-1}(b/a)]}{\sqrt{a^2-b^2}} & a>b\\ -\dfrac{a^n\sin(n\pi/2)}{\sqrt{b^2-a^2}[b+\sqrt{b^2-a^2}]^n} & b>a\end{cases} \quad (57)$$

the singular parts of the stress field, the electric displacement and the magnetic flux can be expressed respectively as follows ($l<x$):

$$\tau=\frac{2\beta_1}{\pi}\sum_{n=1}^{\infty}b_nG_nH_n(x) \quad (58)$$

$$D=\frac{2\beta_2}{\pi}\sum_{n=1}^{\infty}b_nG_nH_n(x) \quad (59)$$

$$B=\frac{2\beta_3}{\pi}\sum_{n=1}^{\infty}b_nG_nH_n(x) \quad (60)$$

where $H_n(x)=-\frac{(-1)^{n-1}l^{2n-1}}{\sqrt{x^2-l^2}[x+\sqrt{x^2-l^2}]^{2n-1}}$.

We obtain the stress intensity factor K as

$$K=\lim_{x\to l^+}\sqrt{2(x-l)}\cdot\tau=-\frac{4\beta_1}{\sqrt{\pi l}}\sum_{n=1}^{\infty}b_n\frac{\Gamma\left(2n-\frac{1}{2}\right)}{(2n-2)!} \quad (61)$$

We obtain the electric displacement intensity factor K^D as

$$K^D=\lim_{x\to l^+}\sqrt{2(x-l)}\cdot D=-\frac{4\beta_2}{\sqrt{\pi l}}\sum_{n=1}^{\infty}b_n\frac{\Gamma\left(2n-\frac{1}{2}\right)}{(2n-2)!}=\frac{\beta_2}{\beta_1}K \quad (62)$$

We obtain the magnetic flux intensity factor K^B as

$$K^B=\lim_{x\to l^+}\sqrt{2(x-l)}\cdot B=-\frac{4\beta_3}{\sqrt{\pi l}}\sum_{n=1}^{\infty}b_n\frac{\Gamma\left(2n-\frac{1}{2}\right)}{(2n-2)!}=\frac{\beta_3}{\beta_1}K \quad (63)$$

5. Numerical calculations and discussion

Adopting the first 10 terms in the infinite series (49), we followed the Schmidt procedure. From the literature [25,26], it can be seen that the Schmidt method performs satisfactorily if the first ten terms of the infinite series (49) are retained. The precision of present solution can satisfy the demands of the practical problem. The constants [3,17,18] of materials-1 are assumed to be that $c_{44}^{(1)}=44.0\,(\mathrm{GPa})$, $e_{15}^{(1)}=5.8\,(\mathrm{C/m^2})$, $\varepsilon_{11}^{(1)}=5.64\times10^{-9}\,(\mathrm{C^2/Nm^2})$, $q_{15}^{(1)}=275.0\,(\mathrm{N/Am})$, $d_{11}^{(1)}=0.005\times10^{-9}\,(\mathrm{Ns/VC})$, $\mu_{11}^{(1)}=-297.0\times10^{-6}\,(\mathrm{Ns^2/C^2})$. The constants of materials-2 are assumed to be that $c_{44}^{(2)}=54.0\,(\mathrm{GPa})$, $e_{15}^{(2)}=7.8\,(\mathrm{C/m^2})$, $\varepsilon_{11}^{(2)}=3.64\times10^{-9}\,(\mathrm{C^2/Nm^2})$, $q_{15}^{(2)}=175.0\,(\mathrm{N/Am})$, $d_{11}^{(2)}=0.008\times10^{-9}\,(\mathrm{Ns/VC})$, $\mu_{11}^{(2)}=-197.0\times10^{-6}\,(\mathrm{Ns^2/C^2})$. The results of the present paper are shown in Figs. 2–4. From the results, the following observations are very significant:

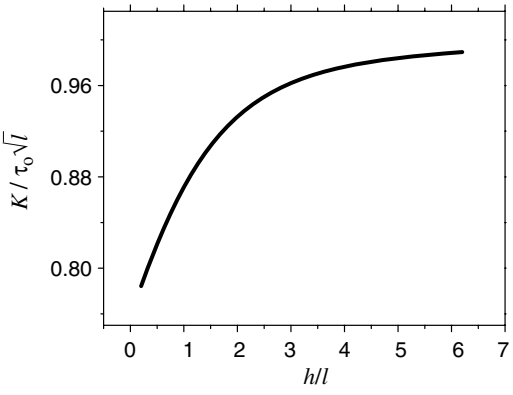

Fig. 2. The stress intensity factor versus h/l (material-1/material-2/material-1).

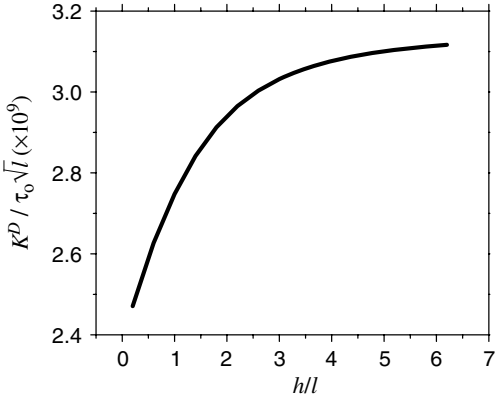

Fig. 3. The electric displacement intensity factor versus h/l (material-1/material-2/material-1).

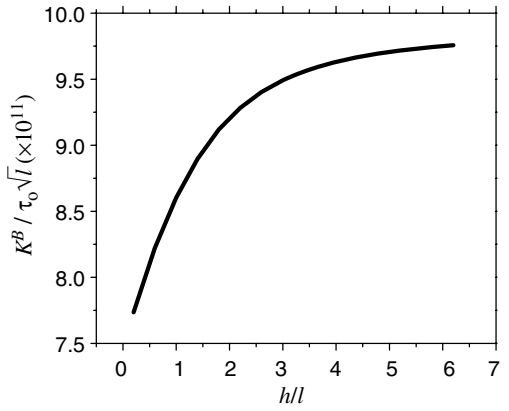

Fig. 4. The magnetic flux intensity factor versus h/l (material-1/material-2/material-1).

(i) The stress, the electric displacement and the magnetic flux intensity factors not only depend on the crack length and the distance between two interface cracks, but also on the properties of the materials and the electro–magneto–elastic coupling effects are obtained as shown in Eqs. (61)–(63). In comparison with the results of Ref. [19], the electro–magneto–elastic coupling effects are considered in the present paper. However, in Ref. [19], only the electro–elastic coupling effects are considered. Certainly, some conclusions are similar with each other in the present paper and in Ref. [19].

(ii) The stress, the electric displacement and the magnetic flux intensity factors increases as the distance between two parallel interfacial cracks increases as shown in Figs. 2–4. This phenomenon is called crack shielding effect as discussed in Ratwani and Gupta's paper [27]. However, the shield effects are very small for $h > 4.0$.

(iii) For $h/l > 4.0$, the stress intensity factors tend to a unit, which is the same as the results of a crack in an infinite plane for the anti-plane shear problem. It can be obtained that the interactions of two parallel interface cracks are very small for $h/l > 4.0$.

(iv) The variations of K, K^D and K^B with h/l have a same tendency as shown in Figs. 2–4. However, the amplitude values of $K/\tau_0\sqrt{l}$, $K^D/\tau_0\sqrt{l}$ and $K^B/\tau_0\sqrt{l}$ are different from each other. The amplitude values of $K^D/\tau_0\sqrt{l}$ and $K^B/\tau_0\sqrt{l}$ are very small as shown in Figs. 3 and 4.

Acknowledgements

The authors are grateful for the financial support by the National Natural Science Foundation of China (10572043, 10572155, 50232030, 10172030), the Natural Science Foundation with Excellent Young Investigators of Hei Long Jiang Province (JC04-08) and the Natural Science Foundation of Hei Long Jiang Province (A0301).

Appendix A

$$[X_1] = \begin{bmatrix} 1 & 0 & 0 \\ \frac{a_1}{a_0} & 1 & 0 \\ \frac{a_2}{a_0} & 0 & 1 \end{bmatrix}, \quad [X_2] = \begin{bmatrix} -1 & 0 & 0 \\ -\frac{a_4}{a_3} & -1 & 0 \\ -\frac{a_5}{a_3} & 0 & -1 \end{bmatrix},$$

$$[X_3] = [X_2], \quad [X_4] = -[X_2], \quad [X_5] = -[X_2],$$

$$[X_6] = -[X_1], \quad [X_7] = \begin{bmatrix} \delta^{(1)} & e_{15}^{(1)} & q_{15}^{(1)} \\ 0 & -\varepsilon_{11}^{(1)} & -d_{11}^{(1)} \\ 0 & -d_{11}^{(1)} & -\mu_{11}^{(1)} \end{bmatrix},$$

$$[X_8] = \begin{bmatrix} -\delta^{(2)} & -e_{15}^{(2)} & -q_{15}^{(2)} \\ 0 & \varepsilon_{11}^{(2)} & d_{11}^{(2)} \\ 0 & d_{11}^{(2)} & \mu_{11}^{(2)} \end{bmatrix}, \quad [X_9] = -[X_8],$$

$$[X_{10}] = -[X_8], \quad [X_{11}] = [X_8], \quad [X_{12}] = [X_7],$$

$$[X_{13}] = [X_8], \quad [X_{14}] = -[X_8],$$

$$[X_{15}] = [X_2] - [X_1][X_7]^{-1}[X_8],$$

$$[X_{16}] = [X_3] - [X_1][X_7]^{-1}[X_9],$$

$$[X_{17}] = [X_4] - [X_6][X_{12}]^{-1}[X_{10}],$$

$$[X_{18}] = [X_5] - [X_6][X_{12}]^{-1}[X_{11}],$$

$$[X_{19}] = [X_{17}] - \mathrm{e}^{-2sh}[X_{18}][X_{16}]^{-1}[X_{15}],$$

$$[X_{20}] = [X_{19}]^{-1}[X_{18}][X_{16}]^{-1}, \quad [X_{21}] = [X_{16}]^{-1}[X_{15}][X_{19}]^{-1},$$

$$[X_{22}] = [X_{16}]^{-1}[X_{15}][X_{19}]^{-1}[X_{18}][X_{16}]^{-1},$$

$$[X_{23}] = -\mathrm{e}^{-sh}[X_{13}][X_{20}] + \mathrm{e}^{-sh}[X_{14}][X_{16}]^{-1} + \mathrm{e}^{-3sh}[X_{14}][X_{22}] = \begin{bmatrix} \delta_{11}(s) & \delta_{12}(s) & \delta_{13}(s) \\ \delta_{21}(s) & \delta_{22}(s) & \delta_{23}(s) \\ \delta_{31}(s) & \delta_{32}(s) & \delta_{33}(s) \end{bmatrix},$$

$$[X_{24}] = [X_{13}][X_{19}]^{-1} - \mathrm{e}^{-2sh}[X_{14}][X_{21}] = \begin{bmatrix} \alpha_{11}(s) & \alpha_{12}(s) & \alpha_{13}(s) \\ \alpha_{21}(s) & \alpha_{22}(s) & \alpha_{23}(s) \\ \alpha_{31}(s) & \alpha_{32}(s) & \alpha_{33}(s) \end{bmatrix}$$

$$g_1(s) = \alpha_{11}(s), \quad g_2(s) = \delta_{11}(s),$$

$$g_3(s) = \delta_{21}(s) + \alpha_{21}(s), \quad g_4(s) = \delta_{31}(s) + \alpha_{31}(s)$$

$$[X_{13}][X_{17}]^{-1} = \begin{bmatrix} \beta_1 & * & * \\ \beta_2 & * & * \\ \beta_3 & * & * \end{bmatrix}$$

References

[1] Wu TL, Huang JH. Closed-form solutions for the magnetoelectric coupling coefficients in fibrous composites with piezoelectric and piezomagnetic phases. Int J Solids Struct 2000;37:2981–3009.

[2] Sih GC, Song ZF. Magnetic and electric poling effects associated with crack growth in $BaTiO_3$–$CoFe_2O_4$ composite. Theor Appl Fract Mech 2003;39:209–27.

[3] Song ZF, Sih GC. Crack initiation behavior in magnetoelectroelastic composite under in-plane deformation. Theor Appl Fract Mech 2003;39:189–207.
[4] Wang BL, Mai YW. Crack tip field in piezoelectric/piezomagnetic media. Eur J Mech A—Solid 2003;22(4):591–602.
[5] Gao CF, Tong P, Zhang TY. Interfacial crack problems in magneto–electroelastic solids. Int J Eng Sci 2003;41(18):2105–21.
[6] Gao CF, Kessler H, Balke H. Fracture analysis of electromagnetic thermoelastic solids. Eur J Mech A—Solid 2003;22(3):433–42.
[7] Spyropoulos CP, Sih GC, Song ZF. Magnetoelectroelastic composite with poling parallel to plane of line crack under out-of-plane deformation. Theor Appl Fract Mech 2003;39(3):281–9.
[8] Liu JX, Liu XL, Zhao YB. Green's functions for anisotropic magnetoelectroelastic solids with an elliptical cavity or a crack. Int J Eng Sci 2001;39(12):1405–18.
[9] Gao CF, Kessler H, Balke H. Crack problems in magnetoelectroelastic solids. Part I: Exact solution of a crack. Int J Eng Sci 2003;41(9):969–81.
[10] Gao CF, Kessler H, Balke H. Crack problems in magnetoelectroelastic solids. Part II: General solution of collinear cracks. Int J Eng Sci 2003;41(9):983–94.
[11] Wang BL, Mai YW. Fracture of piezoelectromagnetic materials. Mech Res Commun 2004;31(1):65–73.
[12] Van Suchtelen J. Product properties: a new application of composite materials. Phillips Res Rep 1972;27:28–37.
[13] Harshe G, Dougherty JP, Newnham RE. Theoretical modeling of 3–0/0–3 magnetoelectric composites. Int J Appl Electromagn Mater 1993;4(2):161–71.
[14] Avellaneda M, Harshe G. Magnetoelectric effect in piezoelectric/magnetostrictive multiplayer (2–2) composites. J Intell Mater Syst Struct 1994;5:501–13.
[15] Nan CW. Magnetoelectric effect in composites of piezoelectric and piezomagnetic phases. Phys Rev B 1994;50:6082–8.
[16] Benveniste Y. Magnetoelectric effect in fibrous composites with piezoelectric and magnetostrictive phases. Phys Rev B 1995;51:16424–7.
[17] Huang JH, Kuo WS. The analysis of piezoelectric/piezomagnetic composite materials containing ellipsoidal inclusions. J Appl Phys 1997;81(3):1378–86.
[18] Li JY. Magnetoelectroelastic multi-inclusion and inhomogeneity problems and their applications in composite materials. Int J Eng Sci 2000;38:1993–2011.
[19] Zhou ZG, Wang B. The behavior of two parallel symmetry permeable interface cracks in a piezoelectric layer bonded to two half piezoelectric materials planes. Int J Solids Struct 2002;39(17):4485–500.
[20] Morse PM, Feshbach H,. Methods of theoretical physics, vol.1. New York: McGraw-Hill; 1958. p. 926.
[21] Yan WF. Axisymmetric slipless indentation of an infinite elastic cylinder. SIAM J Appl Math 1967;15(2):219–27.
[22] Soh AK, Fang DN, Lee KL. Analysis of a bi-piezoelectric ceramic layer with an interfacial crack subjected to anti-plane shear and in-plane electric loading. Eur J Mech A—Solid 2000;19:961–77.
[23] Gradshteyn IS, Ryzhik IM, editors. Table of integrals, series and products. New York: Academic Press; 1980. p. 1035–7.
[24] Erdelyi A, editor. Tables of integral transforms, vol. 1. New York: McGraw-Hill; 1954. p. 34–89.
[25] Zhou ZG, Han HC, Du SY. Investigation of a crack subjected to anti-plane shear by using the non-local theory. Int J Solids Struct 1999;36:3891–901.
[26] Zhou ZG, Bai YY, Zhang XW. Two collinear Griffith cracks subjected to uniform tension in infinitely strip. Int J Solids Struct 1999;36:5597–609.
[27] Ratwani M, Gupta GD. Interaction between parallel cracks in layered composites. Int J Solids Struct 1974;10(7):701–8.